Edelweiss Applied Science and Technology
ISSN: 2576-8484
Vol. 10, No. 3, 541-560
2026
Publisher: Learning Gate
DOI: 10.55214/2576-8484.v10i3.12468

Moderate deficit irrigation improves agronomic performance of quinoa (*Chenopodium quinoa Willd.*) compared to full irrigation in the central highlands of Peru

Esthefany Gavino[1], Dennis Ccopi[1*], Erika Garcia[1], Edilson Requena-Rojas[1], Jose Contreras[2], Richard Solórzano-Acosta[3,4], S. D. Betega[5], Raúl M. Yaranga[6], Samuel Pizarro[1]

[1]Estación Experimental Agraria Santa Ana, Dirección De Servicios Estratégicos Agrarios, Instituto Nacional de Innovación Agraria (INIA), Carretera Saños Grande – Hualahoyo Km 8 Santa Ana, Huancayo, Junín 12006, Peru; dennisccopit@gmail.com (D.C.).
[2]Laboratorio de nutrición animal y evaluation de alimentos (LUNEA), Escuela Profesional de Zootecnia, Universidad Nacional de Huancavelica, Huancavelica 09001, Perú.
[3]Dirección De Servicios Estratégicos Agrarios, Instituto Nacional de Innovación Agraria (INIA), Av. La Molina N° 1981, Lima, 15024, Peru.
[4]Facultad de Ciencias Ambientales, Universidad Científica del Sur (UCSUR), Lima 15024, Peru.
[5]Servicio Nacional de Meteorología e Hidrología del Perú (SENAMHI), Dirección Zonal 11 – Junín, Jirón Tres de Marzo s/n, cuadra 3, Concepción, Junín, Perú.
[6]Andean Ecosystem Research Group, Facultad de Zootecnia, Universidad Nacional del Centro del Perú, Av. Mariscal Castilla 3089, Huancayo, Junin 12002, Peru.

Abstract: This study evaluated the agronomic performance and water productivity of quinoa (Chenopodium quinoa Willd. cv. INIA 433) under three irrigation regimes in the central highlands of Peru: optimal irrigation (Ks = 1.00), moderate deficit (Ks = 0.66), and severe deficit (Ks = 0.49). The experiment combined constant water table lysimeters and field plots, integrating crop coefficient estimation, water balance analysis, and multispectral monitoring (NDVI, NDRE, SRWI) using UAV imagery and ground spectroradiometry. Moderate water stress (Ks = 0.66) significantly improved reproductive performance, producing approximately 8,000 grains per plant compared with ~3,900 grains per plant under optimal irrigation. Grain protein content increased from 4.8% to 6.0%, while evapotranspiration decreased by 37% (from 374.5 to 234.4 mm), markedly improving water use efficiency. In contrast, optimal irrigation promoted maximum vegetative growth (plant height ~110 cm; NDVI 0.7–0.8) but lower reproductive output, whereas severe stress (Ks = 0.49) reduced yield to 4,400 grains per plant and accelerated senescence. Multispectral indices effectively distinguished water stress levels: NDVI reflected canopy vigor, NDRE detected chlorophyll variation, and SRWI captured plant water status. The results demonstrate that regulated deficit irrigation enhances water productivity and grain quality in quinoa. Maintaining Ks values around 0.65–0.70 appears to optimize yield and resource use efficiency in water-limited Andean agroecosystems.

Keywords: *Andean agriculture, crop coefficient, Deficit irrigation, Multispectral remote sensing, Quinoa, Water productivity, Water stress coefficient.*

1. Introduction

Climate change intensifies water scarcity, representing one of the greatest challenges for global agriculture by impacting crop yield, water availability, and food security [1, 2]. Agriculture consumes approximately 72% of global freshwater resources, yet must produce more food with increasingly limited water supplies in a context marked by unequal distribution and projected population growth exceeding 10.3 billion by 2080 [3-5]. Water stress constitutes one of the main threats to agricultural productivity,

History: Received: 14 January 2026; Revised: 20 February 2026; Accepted: 24 February 2026; Published: 19 March 2026
* Correspondence: dennisccopit@gmail.com

as it represents a complex plant response to water deficit that alters physiological, biochemical, and structural functions, limiting plant growth and yield through mechanisms such as stomatal closure, reduced photosynthesis, and decreased transpiration [6-9]. However, emerging evidence suggests that moderate water deficit, when carefully managed, can enhance water use efficiency and, in some cases, even improve yield and quality parameters compared to full irrigation, challenging traditional irrigation paradigms [10, 11].

Accurate quantification of crop water status is essential for designing management strategies that maintain optimal productivity under water-limited conditions. Monitoring crop evapotranspiration (ETc) through the crop coefficient (Kc), a dimensionless parameter relating ETc to reference evapotranspiration (ETo), is considered one of the most efficient methods for evaluating water requirements and managing irrigation at the field scale [12-14]. In recent years, unmanned aerial vehicles (UAVs) equipped with thermal and spectral sensors have demonstrated high potential for early detection of water stress in crops [15].

In recent years, unmanned aerial vehicles (UAVs) equipped with thermal and spectral sensors have demonstrated high potential for early detection of water stress in crops [15]. Vegetation indices derived from multispectral imagery provide non-destructive assessments of crop physiological status under water-limited conditions. The Normalized Difference Vegetation Index (NDVI) estimates foliage vitality, density, and overall canopy vigor [16], while the Normalized Difference Red Edge Index (NDRE) is particularly sensitive to chlorophyll content and photosynthetic capacity [17]. Additionally, water-sensitive indices such as the Simple Ratio Water Index (SRWI) enable direct assessment of plant water status and stress severity [18]. These spectral tools allow precise identification of physiological and structural changes in plants associated with water deficit conditions throughout the crop cycle.

However, not all water stress is detrimental to crop performance. Regulated deficit irrigation (RDI) strategies, which apply moderate water stress during specific phenological stages, have been shown to improve water use efficiency and enhance certain quality parameters without significantly compromising yield in various crops [10, 11]. The flowering stage represents a critical period where moderate stress can trigger beneficial physiological responses, including enhanced root development, improved resource allocation to reproductive structures, and increased stress tolerance mechanisms. When stress is carefully managed, it can ultimately lead to improved agronomic performance.

In this context, quinoa (Chenopodium quinoa Willd.) emerges as a particularly relevant crop. This highly nutritious pseudocereal is recognized as a functional superfood with promising potential to contribute to global food security and climate change mitigation due to its tolerance to drought, salinity, and extreme temperatures, as well as its nutritional value and ability to grow in marginal environments [19, 20]. Quinoa achieves optimal vegetative development and satisfactory yields between 2000 and 3500 m a.s.l. and maintains good performance under limited water conditions [21]. However, studies in arid and semi-arid regions indicate that its evapotranspiration can be high (1100–1600 mm), highlighting the need for efficient water management strategies to optimize both productivity and water use efficiency [22, 23].

Despite quinoa's recognized stress tolerance, limited research has systematically compared its agronomic performance under full irrigation versus deficit irrigation conditions using precise measurement techniques such as lysimeters and remote sensing. Understanding whether quinoa performs better under moderate water deficit compared to full irrigation could provide valuable insights for developing water-saving irrigation strategies that enhance rather than compromise crop performance, especially in water-scarce highland environments.

Therefore, the present study aims to evaluate the agronomic performance of quinoa (Chenopodium quinoa Willd.) under three water regimes: optimal irrigation, continuous deficit irrigation, and rainfed conditions. Specific objectives include: (1) determining the crop coefficient (Kc) using constant water table lysimeters under optimal and deficit irrigation treatments; (2) monitoring physiological responses through remote sensing technologies using NDVI (canopy vigor), NDRE (chlorophyll content), and SRWI (water status) indices; (3) assessing crop yield, quality parameters, and water use efficiency under

Edelweiss Applied Science and Technology
ISSN: 2576-8484
Vol. 10, No. 3: 541-560, 2026
DOI: 10.55214/2576-8484.v10i3.12468

each treatment; and (4) comparing the agronomic performance between full irrigation and deficit irrigation to identify the most efficient water management strategy. Ryegrass is used as a reference crop for ETo calibration and validation.

This research is framed within the United Nations Sustainable Development Goals (SDGs), particularly SDG 2 "Zero Hunger," by promoting sustainable production of nutritious foods; SDG 13 "Climate Action," by contributing to efficient water management and agricultural adaptation to climate variability; and SDG 12 "Responsible Consumption and Production," fostering rational use of natural resources and adoption of climate-smart agricultural practices [24, 25].

2. Materials and Methods

2.1. Study Area

The research was conducted at the Santa Ana Experimental Station of the National Institute of Agricultural Innovation (INIA), located in the district of El Tambo, Huancayo province, Junín department, in the central highlands of Peru (12°0′42.36″ S, 75°13′17.60″ W; 3303–3325 m a.s.l.) (Figure 1). The climate is characterized by marked seasonality, with a rainy season from November to March, a transitional period from April to October, and a dry season from May to August. Mean annual precipitation is approximately 477 mm, and air temperature ranges from 3.9 to 20.2 °C, with frequent frost occurrence during the dry months [26-28].

Soil characterization was performed through certified laboratory analyses (LABSAF–INIA) using twelve composite samples representative of the experimental site. Soils exhibited predominantly loam to clay loam textures (samples 1-12), with pH values ranging from 6.0 to 6.6, corresponding to slightly acidic to near-neutral conditions. Available phosphorus (Olsen method) ranged from 3.0 to 4.8 mg kg^{-1}, indicating low to moderate availability, while organic matter content varied from 9.4 to 12.1 g kg^{-1}. Electrical conductivity was generally low (2.2–13.0 mS m^{-1}), with one sample at 23.9 mS m^{-1}, confirming the absence of salinity limitations. Exchangeable calcium (8.0–12.8 cmol(+) kg^{-1}) and magnesium (1.8–3.1 cmol(+) kg^{-1}) indicated adequate base saturation for quinoa production.

Edelweiss Applied Science and Technology
ISSN: 2576-8484
Vol. 10, No. 3: 541-560, 2026
DOI: 10.55214/2576-8484.v10i3.12468

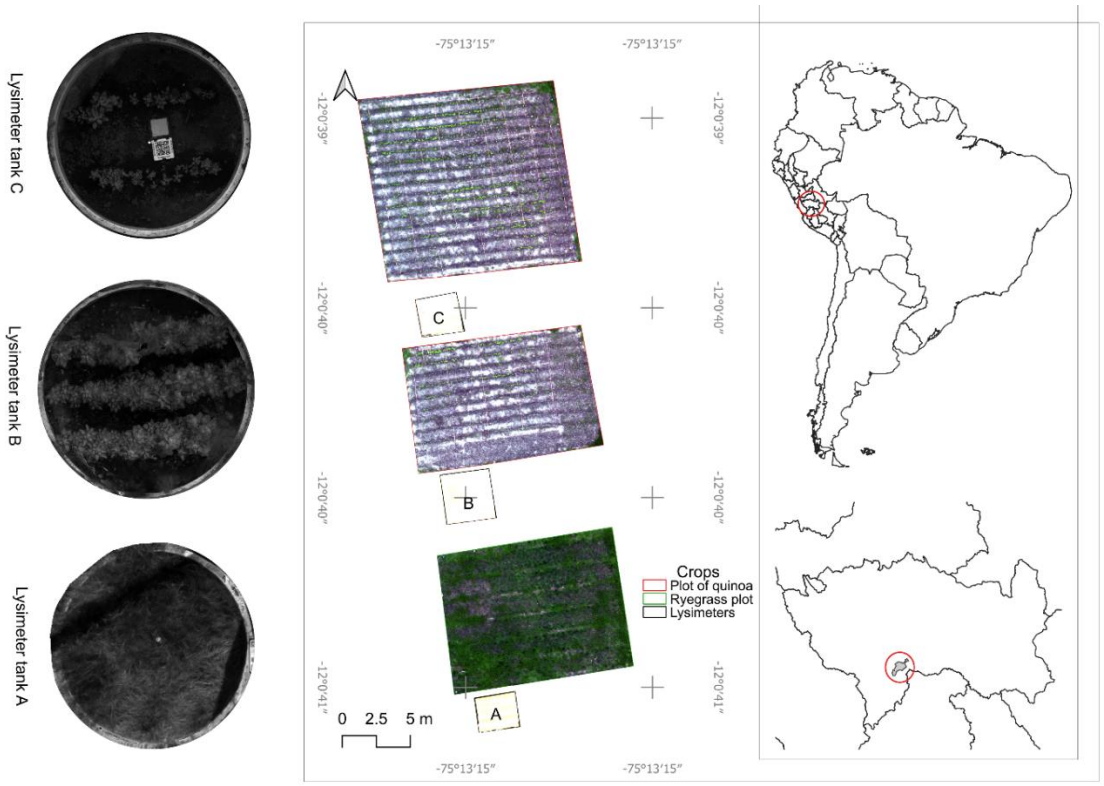

Figure 1.
Location of the Study Area.

2.2. Experimental Design and Treatments

The experiment was established on January 8, 2024, using constant water table lysimeters and field plots. Three cylindrical constant groundwater level lysimeters with a diameter of 1.25 m and a depth of 1.5 m were installed. Each lysimeter was equipped with a water reservoir system connected to maintain a constant water table at 50 cm below the soil surface. To ensure accurate evapotranspiration measurements, lysimeters were covered with transparent rain exclusion shelters positioned 3 m above the canopy to prevent direct precipitation input while allowing air circulation and maintaining ambient light conditions.

Daily evapotranspiration was determined by measuring the volume of water required to maintain the constant water level in the reservoir. Readings were taken twice daily at 7:00 AM and 5:00 PM using a glass graduated cylinder to record the water level in each reservoir. Daily ETc was calculated as the sum of water volume consumed between readings, adjusted for the lysimeter surface area (1.23 m^2).

Three lysimeters were established to evaluate distinct water regimes and calibrate evapotranspiration models. Lysimeter A served as the reference treatment, where ryegrass (Lolium multiflorum Lam.) was maintained under non-limiting water conditions (constant water table at 50 cm depth) throughout the experimental period (January–June 2025) to calibrate and validate meteorologically derived reference evapotranspiration (ETo) estimates. Lysimeter B constituted the optimal irrigation treatment, in which quinoa was cultivated with the water table consistently maintained at 50 cm depth across all phenological stages, representing the upper threshold of water availability and ensuring unrestricted plant growth and development. Lysimeter C comprised the deficit irrigation treatment, where quinoa was subjected to continuous moderate water deficit by maintaining the water table at 80 cm depth, reducing water supply to 60% of optimal consumption, and controlled water restriction via the Z method from emergence to

Edelweiss Applied Science and Technology
ISSN: 2576-8484
Vol. 10, No. 3: 541-560, 2026
DOI: 10.55214/2576-8484.v10i3.12468

physiological maturity, thereby inducing sustained but sub-lethal water stress throughout the growing cycle.

Complementing the lysimeter study, field plots were established under rainfed conditions to evaluate quinoa performance under natural precipitation regimes. Quinoa was grown without supplemental irrigation in plots measuring 5 m × 4 m, with 15 replications. This treatment simulated conventional farmer practices in the region and provided a realistic assessment of crop performance under ambient water-limited conditions.

The quinoa cultivar INIA 433 was sown at a density of 15 kg ha^{-1} with inter-row spacing of 60 cm across all treatments. Soil fertility management consisted of a basal application of 150 kg ha^{-1} N, 120 kg ha^{-1} P_2O_5, and 300 kg ha^{-1} K_2O at sowing [29], supplemented by a top-dressing application of 150 kg ha^{-1} N at the branching stage. All plots were subjected to uniform agronomic practices, including weed control and phytosanitary management. Harvest was conducted on June 18, 2025, when crops achieved physiological maturity, as determined by panicle senescence with over 95% yellow coloration and grain moisture content below 14%.

2.3. Meteorological Conditions During the Growing Season

Meteorological data were recorded throughout the growing season (January–June 2025) using an automated weather station (Davis Vantage 2 Pro) located 100 m from the experimental site. Daily maximum temperature (Tmax), minimum temperature (Tmin), precipitation, relative humidity, wind speed at 2 m height, and solar radiation were measured. Reference evapotranspiration (ETo) was calculated using the FAO-56 Penman-Monteith equation [30].

Figure 2 shows the daily dynamics of maximum temperature (Tmax), minimum temperature (Tmin), precipitation, and reference evapotranspiration (ET_0) during the 2025 cropping season. Tmax exhibited relatively stable thermal behavior, with daily maxima generally ranging between 18 and 25 °C throughout the study period. Tmin showed greater variability, fluctuating between 3 and 10 °C during the main growing season (January–June) and declining to sub-zero values (approximately −5 to −7 °C) in late June and July, corresponding to typical winter frost conditions in the Andean highlands. Precipitation was concentrated between January and March, coinciding with the regional rainy season, with a cumulative rainfall of approximately 320–350 mm, while rainfall intensity and frequency decreased markedly from April to June, resulting in a cumulative precipitation of about 60–80 mm during this latter period. Reference evapotranspiration remained relatively stable across the cropping season, with daily ET_0 values averaging 2.5–3.5 mm d^{-1} and a total cumulative ET_0 of approximately 450–480 mm for the January–June 2025 period.

Edelweiss Applied Science and Technology
ISSN: 2576-8484
Vol. 10, No. 3: 541-560, 2026
DOI: 10.55214/2576-8484.v10i3.12468

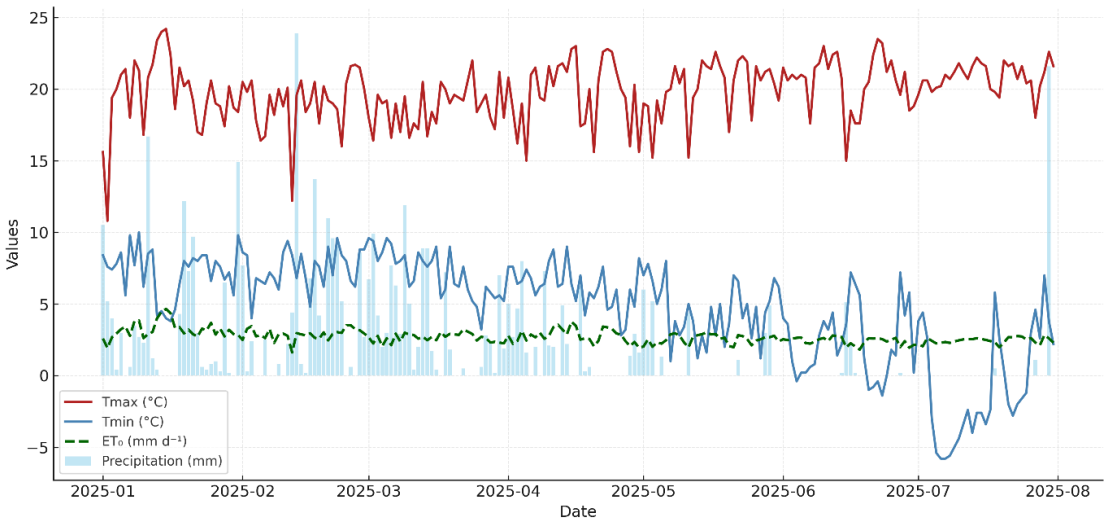

Figure 2.
Seasonal climatic variation and reference evapotranspiration (ETo) during the 2025 cropping season.

2.4. Collection of Agronomic Data

Plant evaluations were conducted at six sampling dates: 70 DAS (vegetative), 91 DAS (branching), 104 DAS (early flowering), 119 DAS (full flowering), 145 DAS (grain filling), and 162 DAS (physiological maturity). A total of 480 individually tagged plants were monitored across all treatments, enabling detailed tracking of physiological and agronomic responses throughout the crop cycle.

2.5. Morphological and Physiological Parameters

Chlorophyll content was assessed using a portable SPAD-502 Plus meter (Konica Minolta, Japan), with readings taken from fully expanded leaves located at mid-canopy height. Plant height was measured from the soil surface to the apex of the highest leaf using a graduated metric ruler (±0.1 cm precision). Leaf number was recorded by counting all fully expanded leaves per plant. Panicle length was measured from the base to the apex of the primary inflorescence at physiological maturity.

Midday leaf water potential (Ψ_{leaf}) was determined using a Scholander-type pressure chamber (Model 600, PMS Instrument Company, USA). Selected fully expanded leaves were enclosed in reflective bags for 5 minutes to equilibrate vapor pressure, then excised with approximately 3 cm of petiole remaining for chamber insertion. Measurements were conducted between 11:00 AM and 1:00 PM under clear sky conditions.

Soil water status was monitored using granular matrix sensors (Watermark 200SS, Irrometer Company, USA) installed at 15 cm depth in each experimental unit. Soil water tension (kPa) was recorded twice daily at 7:00 AM and 5:00 PM throughout the crop cycle, coinciding with lysimeter water consumption measurements.

2.6. Biomass and Yield Components

At physiological maturity, total aboveground biomass was harvested from 30 plants per treatment, separated into vegetative and reproductive fractions, and oven-dried at 70°C for 72 hours until constant weight. Leaf area was determined by scanning fresh leaves alongside a scale reference ruler using a flatbed scanner. Digital images were processed and analyzed in R software [31] using a k-means clustering algorithm for image segmentation to separate leaf tissue from the background. Leaf area (cm^2) was calculated by converting pixel counts to actual area using the scale reference calibration.

Grain yield was determined by hand-threshing panicles from 75 plants per lysimeter and per field plot, with grain moisture adjusted to 12% wet basis. Yield per unit area (kg ha^{-1}) was calculated based on

Edelweiss Applied Science and Technology
ISSN: 2576-8484
Vol. 10, No. 3: 541-560, 2026
DOI: 10.55214/2576-8484.v10i3.12468

a planting density of 35 plants m^{-2}. Thousand-grain weight (TGW) was determined from five replicate counts of 1000 grains per treatment using a precision analytical balance (±0.001 g). Grain number per plant was calculated as: (individual plant grain weight / TGW) × 1000.

Grain protein content was analyzed at the National University of Huancavelica, Animal Nutrition and Feed Evaluation Laboratory using the Dumas method. Crude protein (CP) was assessed with the Dumas nitrogen determination technique employing a Dumas-01 model manufactured by FP 528, Leco, St. Joseph, MI, USA. Additionally, CP was calculated using a 6.25 nitrogen-to-protein conversion factor [32].

2.7. Remote Sensing and Spectral Data Analysis

Aerial multispectral imagery was acquired at six dates throughout the crop cycle: 70, 91, 104, 141, 162, and 170 days after sowing (DAS), with the final flight conducted post-harvest to document canopy senescence. Flights were performed using a DJI Phantom 4 RTK UAV equipped with a Parrot Sequoia+ multispectral sensor capturing four spectral bands: green (550 nm), red (660 nm), red-edge (735 nm), and near-infrared (790 nm). All flights were conducted at 30 m altitude with 80% frontal and lateral overlap at 4 m s^{-1} between 11:00 AM and 1:00 PM under clear sky conditions. Radiometric calibration was performed before each flight using the Parrot Sequoia calibrated reflectance panel.

Complementary ground-based spectral measurements were acquired using a FieldSpec HandHeld 2 spectroradiometer (ASD Inc., USA) operating across 325–1075 nm with 1.5 nm sampling interval, 3.5 nm spectral resolution (FWHM at 700 nm), and 25° field of view. Measurements were taken at canopy level on the same dates as UAV flights, with white reference calibration performed using a Spectralon® panel before each measurement session.

Multispectral orthomosaics were generated using Pix4Dmapper Pro v4.8.4 (Pix4D, Switzerland), incorporating ground control points to ensure geometric and radiometric accuracy. Spectral data processing and analysis were performed in RStudio v4.4.1 [31] using the terra package [33] with QGIS v3.18.14 [34] for image editing and layer vectorization.

Three vegetation indices were calculated to assess canopy vigor, chlorophyll content, and water status: the Normalized Difference Vegetation Index (NDVI):

$$NDVI = (\rho NIR - \rho Red) / (\rho NIR + \rho Red)$$

Normalized Difference Red Edge Index (NDRE):

$$NDRE = (\rho NIR - \rho RedEdge) / (\rho NIR + \rho RedEdge)$$

Simple Ratio Water Index (SRWI):

$$SRWI = \rho NIR / \rho SWIR$$

An NDVI-based mask (threshold > 0.2) was applied to isolate active vegetation and eliminate soil background. For each treatment, zonal statistics (mean, median, minimum, maximum) were computed from valid pixels, with outliers removed using an adaptive interquartile range filter. Temporal trends were visualized using LOESS smoothing to evaluate phenological patterns in canopy development, chlorophyll dynamics, and water status throughout the crop cycle.

2.8. Evaluation of the Water Stress Coefficient (Ks)

The reference evapotranspiration (ET_0) was calculated using the Penman–Monteith equation, which integrates the energetic and aerodynamic components of the water balance. This formulation incorporates net radiation, air temperature, wind speed, and vapor pressure deficit, allowing the estimation of atmospheric water demand for a well-watered reference surface [35].

In Equation (1) of the FAO-56 Penman–Monteith method [30], reference evapotranspiration (ET_0) represents the atmospheric demand for water from a well-watered and fully vegetated reference surface. Net radiation (R_n) denotes the energy available at the crop surface after subtracting reflected shortwave radiation and longwave radiative losses. Soil heat flux (G) corresponds to the energy transferred to or from the soil profile, typically considered negligible at a daily scale. Mean air temperature (T) and wind

Edelweiss Applied Science and Technology
ISSN: 2576-8484
Vol. 10, No. 3: 541-560, 2026
DOI: 10.55214/2576-8484.v10i3.12468

speed at 2 m height (u_2) determine the capacity of the air to transport water vapor, while the vapor pressure deficit ($e_s - e_a$) reflects the humidity gradient between the canopy surface and the atmosphere. The slope of the saturation vapor pressure curve (Δ) and the psychrometric constant (γ) regulate the relationship between temperature, pressure, and humidity, balancing the energetic and aerodynamic components of the evapotranspiration process [35, 36].

$$ET_o = \frac{0.408\Delta\,(R_n - G) + \gamma \frac{900}{T+273} + u_2(e_s - e_a)}{\Delta + \gamma\,(1 + 0.34\,u_2)} \quad (1)$$

Crop evapotranspiration (ETc) was subsequently obtained by multiplying ET_0 by the crop coefficient (Kc), which was adjusted according to the phenological stages of quinoa—initial, development, mid-season, and late-season. This relationship allows quantifying the crop's potential water demand under optimal soil moisture conditions [30, 37], as expressed in Equation (2):

$$ET_c = K_c\, x\, ET_o \quad (2)$$

The crop coefficient (Kc) represents the relationship between the transpiration of a specific crop and that of the reference surface. Its value varies according to the phenological stages: initial (Kc_ini), development, mid-season (Kc_mid), and late-season (Kc_end), reflecting changes in canopy cover, leaf area, and overall crop structure [30].

In the third stage, the water stress coefficient (Ks) was estimated from soil water content and the fraction of readily available water (p). The value of Ks ranges from 1 (no stress) to 0 (severe stress), reflecting the crop's ability to maintain transpiration under limited soil moisture conditions, as expressed in Equation [30].

$$K_s = \begin{cases} 1 \\ \frac{TAW - D_r}{TAW - RAW} \end{cases} \quad (3)$$

The water stress coefficient (Ks) quantifies the relative reduction in transpiration caused by soil water deficit. This parameter depends on root-zone depletion (D_r), total available water (TAW), and readily available water (RAW = p × TAW), where p is the fraction of water that the crop can extract without experiencing stress. TAW corresponds to the amount of water held in the soil between field capacity and the permanent wilting point [30, 37].

The actual crop evapotranspiration (ETc_act) was finally calculated as the product of ETc and Ks, and incorporated into a simplified "bucket" soil water balance model, where root-zone water storage was updated daily based on effective precipitation, deep percolation, and evapotranspiration losses. This framework allowed quantifying the crop's effective water use and the magnitude of water stress throughout the phenological cycle [30, 38] as expressed in Equations (4) and (5):

$$ET_{cact} = K_s\, x\, ET_c \quad (4)$$

$$S_t = S_{t-1} + P_{eff} - ET_{cact} - DP \quad (5)$$

S_t represents soil water storage on day t, P_{eff} is the effective precipitation that replenishes the root zone, ET_{cact} is the actual evapotranspiration determined by the interaction between atmospheric demand and soil water availability, and DP denotes deep percolation, which corresponds to water exceeding the

Edelweiss Applied Science and Technology
ISSN: 2576-8484
Vol. 10, No. 3: 541-560, 2026
DOI: 10.55214/2576-8484.v10i3.12468

soil's storage capacity and being lost through drainage. These variables allow evaluating soil water dynamics and the crop's response to water stress throughout each development stage [38].

2.9. Statistical Analysis and Water Modeling of the Crop

The procedure integrated the statistical analysis and soil water balance of quinoa under different water stress levels. Data were processed in RStudio (R v4.4.1) [31] through an automated workflow that included data cleaning, balanced subsampling, one-way ANOVA, Tukey HSD comparisons, and the estimation of reference evapotranspiration (ET_0) and actual crop evapotranspiration (ETc) using the FAO-56 Penman–Monteith method. Climatic variables related to radiation, vapor pressure, wind, and energy balance were incorporated, adjusting atmospheric pressure to the site elevation (3,298 m) and using an albedo of 0.23. The crop coefficient (Kc) curve was combined with ET_0 to obtain potential evapotranspiration (ETc_{po}), and a bucket-type soil water balance model was used to estimate the stress coefficient (Ks) and actual evapotranspiration (ETc_act), considering $\theta_{FC} = 0.30$, $\theta_{WP} = 0.15$, and $p = 0.55$. All processing and visualization were performed in RStudio using the packages readxl, openxlsx, dplyr, ggplot2, lubridate, emmeans, multcomp, janitor, tidyr, stringr, forcats, and rstudioapi [39-43].

3. Results

3.1. Seasonal Water Balance and Water Stress Quantification

Figure 3 illustrates the seasonal water balance dynamics and the progressive development of water stress under rainfed field conditions (Ks = 0.66). The cumulative water budget (Figure 3a) reveals that total reference evapotranspiration (ETo = 520.6 mm) substantially exceeded effective rainfall (365.4 mm), generating a cumulative water deficit of 155.2 mm over the growing season. This deficit was partially compensated by depletion of initial soil water reserves (60 mm), while substantial deep percolation losses (177 mm) occurred primarily during the wet season (January–March) when rainfall intensity exceeded soil infiltration capacity, Midday leaf water potential and storage approached field capacity.

Daily actual crop evapotranspiration (ETc_actual = 234.4 mm; Figure 3b) exhibited a characteristic bell-shaped seasonal pattern, gradually increasing during vegetative establishment (January–March), reaching maximum values exceeding 4 mm d^{-1} during flowering and early grain filling (late April–early May), then declining sharply as soil water depletion intensified and plants approached physiological maturity. The ETc_actual represented only 45% of potential crop water demand (Kc = 0.45), indicating substantial water limitation throughout the cycle.

Effective rainfall distribution (Figure 3c) was highly concentrated in the early season (January–March: 300 mm), with sporadic events in April (~50 mm) and virtually no precipitation from May through harvest. This temporal mismatch between water supply and crop demand severely limited water availability during the critical reproductive and grain-filling phases, when quinoa's water requirements were highest.

Root zone soil water storage (Figure 3d) remained near field capacity (60 mm) during the vegetative phase due to frequent rainfall recharge. However, storage declined progressively from mid-April onward as atmospheric evaporative demand exceeded precipitation inputs. By late May, soil moisture approached the wilting point (<5 mm available water), Forcing stomatal closure and dramatically reducing transpiration, this severe late-season water deficit (Ks declining from 0.8 in April to less than 0.4 in June) imposed moderate-to-high cumulative stress (seasonal Ks = 0.66), Contrasting sharply with the non-limiting conditions (Ks = 1.00) maintained continuously in the optimally irrigated lysimeter treatment (LB).

Edelweiss Applied Science and Technology
ISSN: 2576-8484
Vol. 10, No. 3: 541-560, 2026
DOI: 10.55214/2576-8484.v10i3.12468

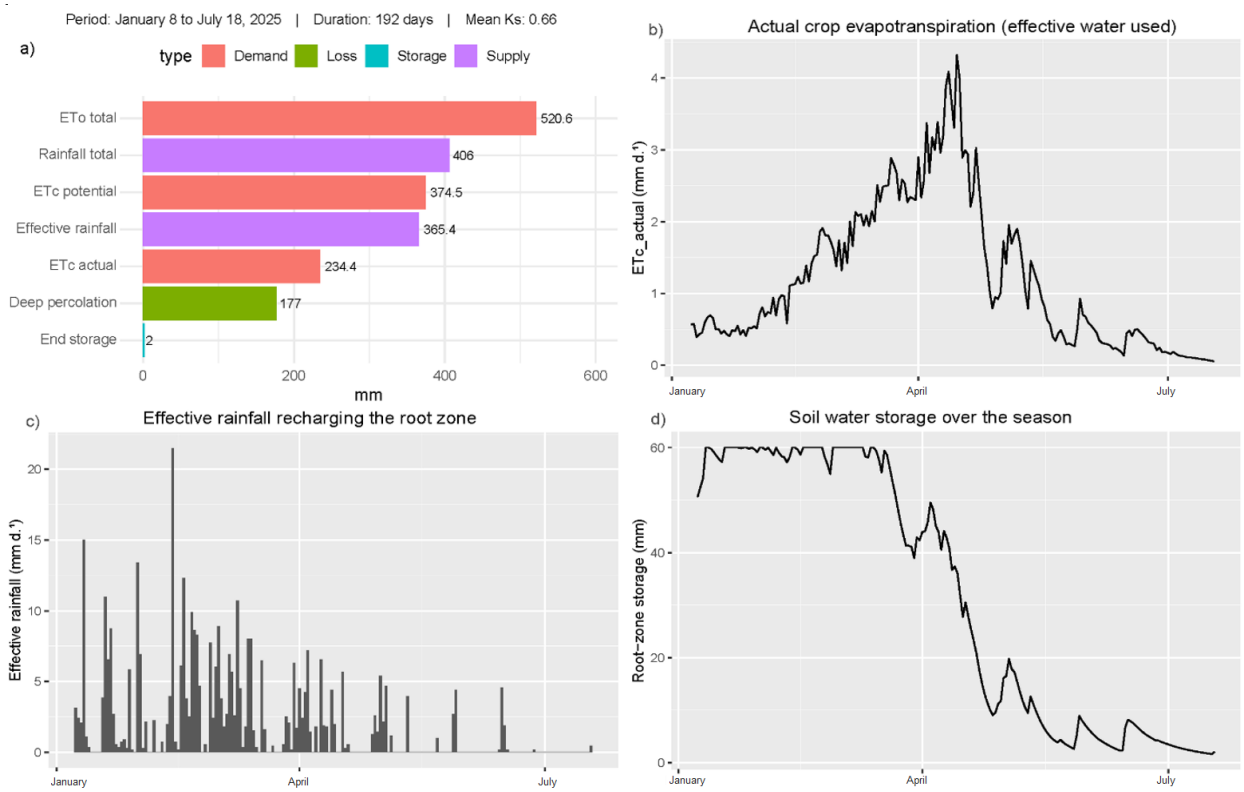

Figure 3.
Seasonal water balance components and water stress development under rainfed conditions (Ks = 0.66). (a) Cumulative water budget showing ET_o, ETc, effective rainfall, deep percolation, and changes in soil water storage; (b) Daily actual crop evapotranspiration (ETc_actual) showing peak demand during flowering; (c) Effective rainfall distribution highlighting early-season concentration and late-season deficit; (d) Progressive depletion of root zone soil water storage from field capacity to near wilting point.

Table 1 presents the water stress coefficient (Ks), actual crop evapotranspiration (ETc), and observed crop coefficient (Kc) under three irrigation treatments. In the LB (optimal irrigation) treatment, plants experienced no water stress (Ks = 1.00), achieving maximum ETc of 374.5 mm and an observed Kc of 0.72, representing crop water demand under non-limiting conditions.

Under field (rainfed) conditions, moderate water stress (Ks = 0.66) reduced ETc to 234.4 mm and the observed Kc to 0.45, indicating intermittent water limitation associated with natural rainfall variability and progressive soil water depletion. In the LC (deficit irrigation) treatment, severe water stress (Ks = 0.49) substantially constrained ETc to 183.1 mm (49% of optimal), with the observed Kc declining to 0.35, reflecting prolonged water deficit that significantly reduced transpiration and effective crop water use throughout the growing cycle.

Table 1.
Water stress coefficient (Ks), crop evapotranspiration (ETc), and crop coefficient (Kc) under different irrigation treatments.

Treatment	Ks	ETc (mm)	Observed Kc (ETc/ETo*)	Stress Level	Water Condition
LB – Optimal	1.00	374.5	0.72	None	Full irrigation, no limitation
Field – Rainfed	0.66	234.4	0.45	Moderate	Natural rainfall, intermittent stress
LC – Deficit	0.49	183.1	0.35	Severe	Prolonged water deficit

Note: *Reference evapotranspiration (ETo) = 520.6 mm for the growing season (January 8 – June 18, 2025).

Edelweiss Applied Science and Technology
ISSN: 2576-8484
Vol. 10, No. 3: 541-560, 2026
DOI: 10.55214/2576-8484.v10i3.12468

3.2. Morphophysiological Response to Water Stress

3.2.1. Vegetative Growth and Canopy Development

Figure 4 illustrates the vegetative growth dynamics of quinoa under three irrigation treatments throughout the growing cycle: optimal irrigation (LB, Ks = 1.00), rainfed field conditions (Ks = 0.66), and deficit irrigation (LC, Ks = 0.49).

Plant height and leaf number showed clear treatment differentiation from early stages onward. Optimal irrigation (Ks = 1.00) consistently produced the tallest plants, reaching a maximum height of approximately 110 cm at 119 DAS, followed by rainfed conditions (Ks = 0.66, 75 cm) and deficit irrigation (Ks = 0.49, 75 cm). Leaf number followed a similar pattern, with optimal irrigation maintaining the highest leaf counts throughout the cycle. Treatment differences became more pronounced after 119 DAS (flowering stage), where water stress markedly limited vertical growth and accelerated leaf senescence, particularly under severe deficit conditions.

Panicle length development began at 91 DAS, with all treatments showing progressive elongation through reproductive stages. At mid-flowering (119 DAS), severe deficit irrigation (Ks = 0.49) showed significantly reduced panicle length compared to optimal (Ks = 1.00) and rainfed (Ks = 0.66) treatments. However, by late grain filling and physiological maturity (145–162 DAS), panicle length converged across all treatments, reaching approximately 45–55 cm with no significant differences ($p > 0.05$).

SPAD chlorophyll index exhibited peak values at 104–119 DAS across all treatments, with rainfed plants (Ks = 0.66) showing the highest readings (54), suggesting enhanced chlorophyll concentration as an osmotic adjustment mechanism under moderate stress. All treatments showed declining SPAD values toward maturity (162 DAS), consistent with natural leaf senescence.

Edelweiss Applied Science and Technology
ISSN: 2576-8484
Vol. 10, No. 3: 541-560, 2026
DOI: 10.55214/2576-8484.v10i3.12468

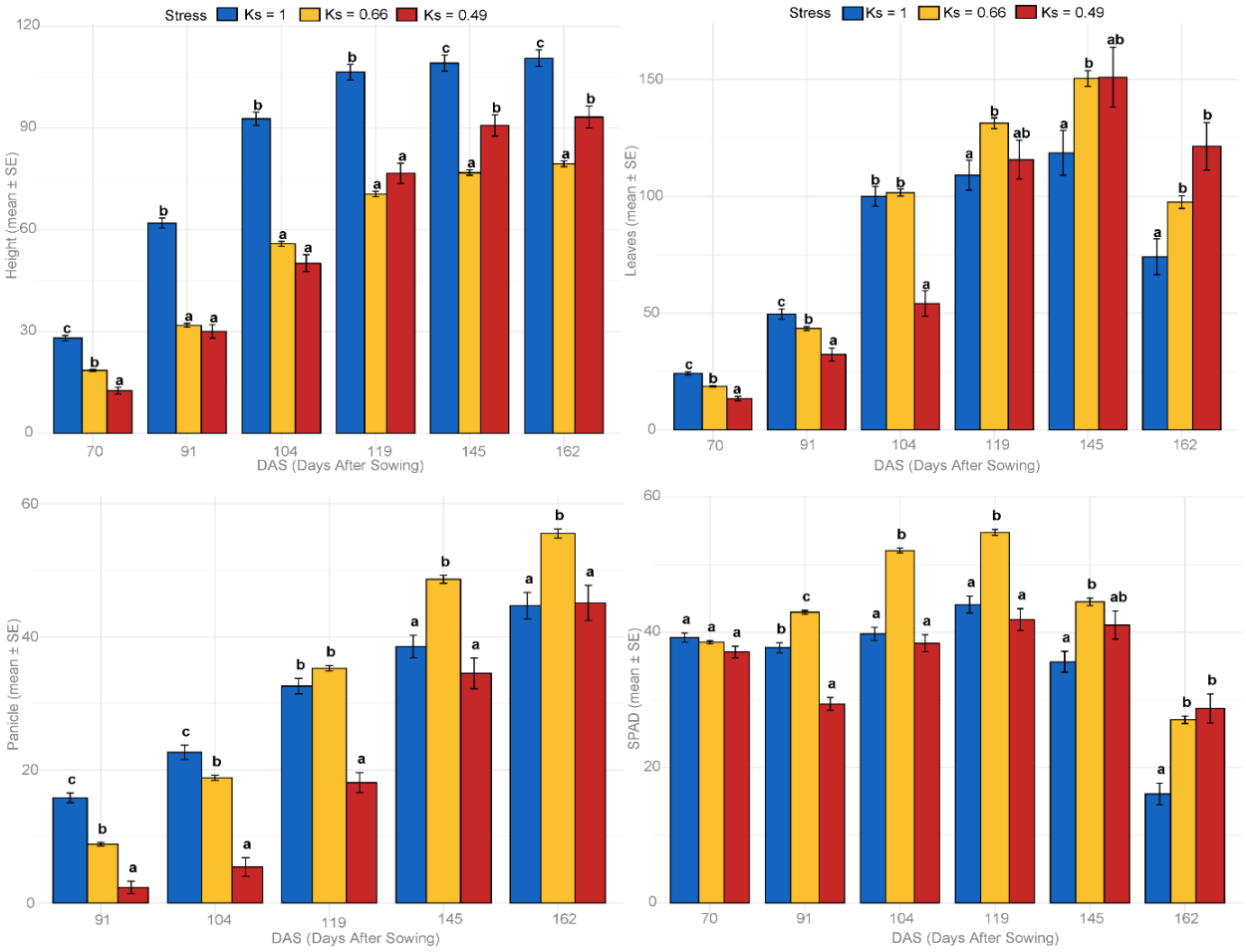

Figure 4.
Vegetative growth dynamics of quinoa (*Chenopodium quinoa* Willd.) under three irrigation treatments: optimal (LB, Ks = 1.00, blue), rainfed (Ks = 0.66, yellow), and deficit (LC, Ks = 0.49, red). **(a)** Plant height, **(b)** Number of leaves; **(c)** Panicle length; **(d)** SPAD chlorophyll index. Different letters indicate significant differences ($p < 0.05$) among treatments at each sampling date (Tukey HSD test). Error bars represent the standard error of the mean (n = 80 plants per treatment).

3.2.2. Reproductive Performance and Grain Quality

Figure 5 presents reproductive output and grain quality under three irrigation treatments. Total grain weight per plant (Figure 5a) was highest under rainfed conditions (Ks = 0.66, 27 g plant^{-1}), approximately doubling that of optimal irrigation (Ks = 1.00, 13 g plant^{-1}) and severe deficit (Ks = 0.49, 13 g plant^{-1}, $p < 0.05$). This increase resulted from substantially higher grain number (Figure 5c): 7,700 grains per plant under Ks = 0.66 compared to approximately 3,400 (Ks = 1.00) and 4,400 (Ks = 0.49). Grain protein content (Figure 5b) followed a similar pattern, with rainfed conditions achieving about 6.0%, significantly exceeding optimal irrigation (4.8%) and severe deficit (3.7%, $p < 0.05$).

Edelweiss Applied Science and Technology
ISSN: 2576-8484
Vol. 10, No. 3: 541-560, 2026
DOI: 10.55214/2576-8484.v10i3.12468

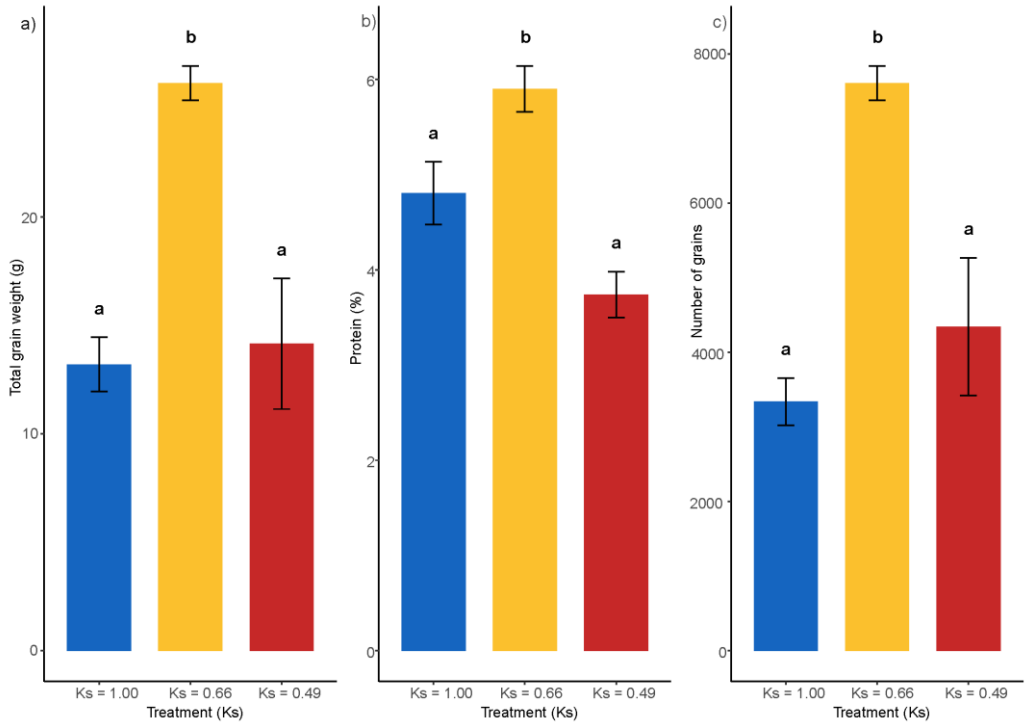

Figure 5.
Reproductive performance and grain quality. (a) Total grain weight (g plant^{-1}); (b) Grain protein (%); (c) Number of grains per plant. Blue: Ks = 1.00; Yellow: Ks = 0.66; Red: Ks = 0.49. Different letters indicate significant differences ($p < 0.05$, Tukey HSD). Error bars: SE (n = 80).

3.3. Spectral Response and Vegetation Indices Under Water Stress

Figure 6 presents the spectral dynamics and vegetation indices of quinoa under three irrigation treatments throughout the growing cycle. Panel a shows NDVI temporal evolution visualized through lysimeter imagery from 68 to 162 DAS. At early vegetative stages (68 DAS), optimal irrigation (Ks = 1.00) exhibited uniform, vigorous canopy cover, while moderate (Ks = 0.66) and severe (Ks = 0.49) stress treatments showed reduced development and localized stress patches. During peak vegetative growth (93–141 DAS), Ks = 1.00 maintained high NDVI values, whereas stressed treatments displayed progressive canopy reduction and spatial heterogeneity. By 162 DAS, all treatments showed declining NDVI corresponding to senescence, with stress-accelerated deterioration evident in Ks = 0.49.

Spectral signatures (Figure 6b, 400–1000 nm) at four key growth stages (92, 126, 148, and 166 DAS) confirmed these visual patterns. Optimal irrigation (Ks = 1.00) maintained high near-infrared reflectance (700–900 nm) and strong red absorption (600–680 nm) throughout the cycle, indicating sustained chlorophyll content and canopy vigor. Stressed treatments showed progressive chlorophyll loss (reduced red absorption) and decreased NIR reflectance, particularly at 148 and 166 DAS. The ryegrass reference crop exhibited lower overall reflectance due to denser leaf structure.

The temporal evolution of key indices (Figure 6c) revealed distinct physiological patterns: NDRE (chlorophyll) peaked at approximately 119 DAS across treatments, with Ks = 1.00 maintaining the highest values (~0.32). NDVI (vigor) showed maximum differentiation during 93–141 DAS, following the pattern Ks = 1.00 > Ks = 0.66 > Ks = 0.49, with peak values around 0.7–0.8 for optimal irrigation. SRWI (water status) demonstrated the highest values under severe stress (Ks = 0.49, reaching ~8 at late stages), confirming progressive water deficit, while Ks = 1.00 maintained lower, more stable values (~4–5). These spectral parameters effectively differentiated quinoa physiological responses to water availability throughout the crop cycle.

Edelweiss Applied Science and Technology
ISSN: 2576-8484
Vol. 10, No. 3: 541-560, 2026
DOI: 10.55214/2576-8484.v10i3.12468

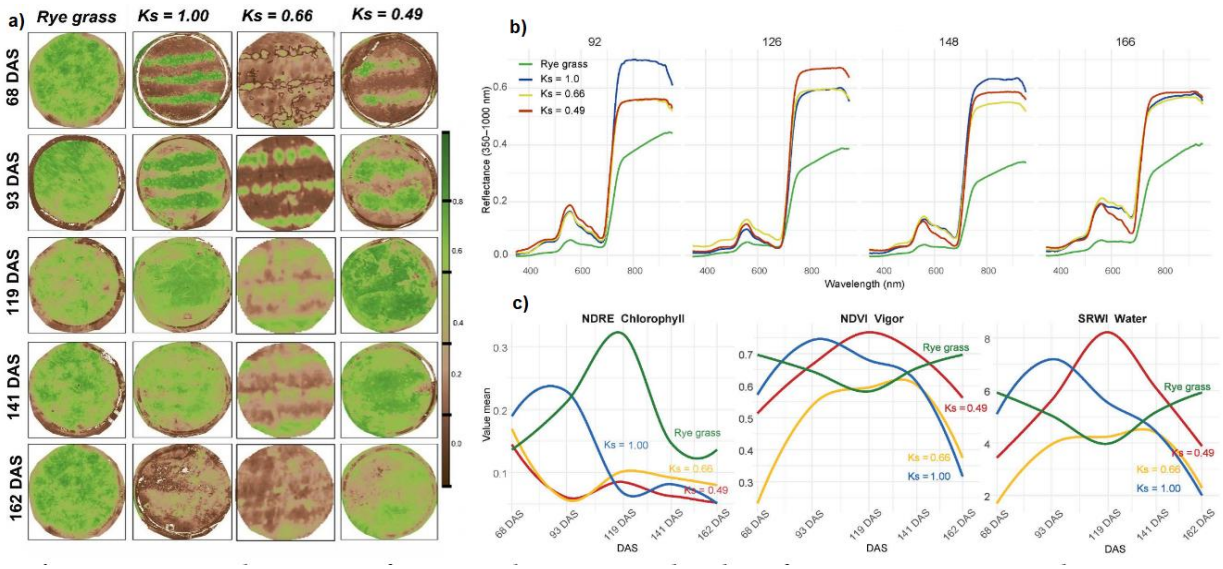

Figure 6.
Spectral response and vegetation indices under water stress. **(a)** NDVI temporal evolution in lysimeters at 68, 93, 119, 141, and 162 DAS; **(b)** Spectral signatures (400–1000 nm) at 92, 126, 148, and 166 DAS; **(c)** Temporal variation of NDRE (chlorophyll), NDVI (vigor), and SRWI (water status) indices throughout the growing season. Gray: Ryegrass; Blue: Ks = 1.00; Yellow: Ks = 0.66; Red: Ks = 0.49.

4. Discussions

4.1. Enhanced Reproductive Performance Under Moderate Water Deficit

This study demonstrates that quinoa (*Chenopodium quinoa* Willd. cv. INIA 433) exhibits a non-linear response to water availability in the central highlands of Peru, with moderate stress producing superior reproductive output compared to optimal irrigation. Rainfed field conditions (Ks = 0.66) generated approximately 8,000 grains per plant, more than double that achieved under optimal lysimeter irrigation (Ks = 1.00, 3,900 grains per plant), while simultaneously increasing grain protein content from 4.8% to 6.0%. This response, where moderate stress surpasses performance under non-limiting conditions, challenges conventional irrigation paradigms and demonstrates quinoa's remarkable capacity to optimize reproductive allocation under intermediate water limitation [21, 22].

The mechanisms underlying this enhanced reproductive output appear to involve coordinated shifts in resource allocation under intermediate water deficit. While optimal irrigation promoted maximum vegetative growth (plant height: 110 cm, leaf number: 150), reflecting the high drought tolerance reported for quinoa [19, 23], this vegetative investment did not translate into proportional reproductive success. Moderate stress reduced vegetative biomass but dramatically increased reproductive sink number, suggesting water limitation triggered a developmental shift prioritizing reproduction over vegetative expansion. This adaptive mechanism is consistent with observations in arid and semi-arid environments where quinoa maintains or even enhances performance under moderately restricted water availability [21, 22].

The concurrent protein increase under moderate stress suggests enhanced nitrogen remobilization from vegetative tissues to grains, consistent with previous findings showing that intermediate water restriction promotes significant increases in protein content through physiological adjustments in nitrogen metabolism and grain filling. Stikic et al. [44] and Yang et al. [45] support this. This combined improvement in grain number and quality offers a critical advantage for food security in water-scarce regions.

In contrast, severe deficit (Ks = 0.49) markedly reduced growth, panicle elongation, and biomass accumulation, aligning with adverse physiological effects documented in crops exposed to water deficit,

including reduced photosynthesis, altered water balance, and decreased leaf area [7, 8]. Severe stress produced only 4,400 grains per plant and the lowest protein content (3.7%), indicating that stress beyond critical thresholds overwhelms compensatory mechanisms. The narrow window between beneficial moderate stress (Ks = 0.66) and detrimental severe stress (Ks = 0.49) emphasizes the importance of precise water management.

4.2. Morphophysiological and Spectral Responses to Progressive Water Deficit

Progressive water reduction induced predictable morphophysiological changes: plant height decreased from 110 cm (Ks = 1.00) to 75 cm (Ks = 0.66, 0.49). Leaf number declined, and SPAD chlorophyll values decreased under stress, reflecting the high sensitivity of expansive growth to declining water potential [46]. However, panicle length converged across treatments by maturity despite significant differences at mid-flowering (119 DAS), indicating compensatory growth prioritizing reproductive structures—consistent with stress adaptation mechanisms in quinoa [47].

SPAD chlorophyll peaked at 104-119 DAS across treatments, with moderate stress (Ks = 0.66) showing the highest readings (~54), suggesting enhanced chlorophyll concentration per unit leaf area as an osmotic adjustment optimizing light capture capacity in a reduced canopy, a response documented in stress-tolerant quinoa genotypes [48]. The accelerated senescence under severe deficit (Ks = 0.49) reflected photosynthetic collapse when stress exceeded buffering thresholds, consistent with reports where water deficit accelerates leaf senescence and limits photoassimilate accumulation in sensitive genotypes [49].

Multispectral indices effectively captured stress progression throughout the crop cycle. NDVI dynamics paralleled morphophysiological patterns: optimal irrigation maintained high values (0.7-0.8) during 93-141 DAS, moderate stress showed intermediate stability, and severe deficit exhibited a progressive decline. Spectral signatures (400-1000 nm) confirmed these patterns through characteristic red absorption (600-680 nm) and NIR reflectance (700-900 nm) changes, with stressed treatments showing progressive chlorophyll loss and structural deterioration. Water stress rapidly affects reflectance in red and NIR bands due to chlorophyll degradation and cellular contraction, with NIR reflectance extremely sensitive to turgor and cell volume loss [50-52].

NDRE proved particularly sensitive to chlorophyll dynamics, peaking at 119 DAS (0.32) and providing early stress detection before visible symptoms. SRWI showed dramatic differentiation, with severe stress reaching 8 versus 4-5 for optimal irrigation. The integration of NDVI (canopy vigor), NDRE (chlorophyll), and SRWI (water status) provided complementary information, distinguishing moderate stress that maintained function from severe stress causing irreversible decline, offering potential for precision irrigation management based on real-time physiological monitoring [18].

4.3. Water Stress Coefficient as an Integrative Metric and Management Tool

The water stress coefficient (Ks) effectively integrates soil water availability and crop performance. The three levels (1.00, 0.66, 0.49) represent distinct physiological states: optimal hydraulic function, moderate stress with partial stomatal limitation, and severe stress approaching hydraulic failure. Superior performance at Ks = 0.66 indicates operation within an "adaptive zone" where quinoa successfully regulates physiological processes without entering metabolic decline, corresponding to the gradually declining Ks curve where compensatory mechanisms offset water limitation [30, 53].

The relationship between Ks and crop coefficient (Kc) illustrates substantial water productivity improvements. Optimal irrigation (Ks = 1.00) showed Kc = 0.72 (ETc = 374.5 mm), while moderate stress (Ks = 0.66) reduced ETc to 234.4 mm (Kc = 0.45)—achieving 37% water savings while doubling grain production, demonstrating the potential for deficit irrigation to enhance water productivity in quinoa [54]. Severe stress (Ks = 0.49) further reduced ETc to 183.1 mm (Kc = 0.35) but compromised yield, demonstrating diminishing returns beyond optimal deficit thresholds, consistent with nonlinear crop responses to progressive water limitation [55].

Edelweiss Applied Science and Technology
ISSN: 2576-8484
Vol. 10, No. 3: 541-560, 2026
DOI: 10.55214/2576-8484.v10i3.12468

4.4. Implications for Water-Scarce Andean Agriculture

These findings have direct implications for irrigation management in water-limited Andean systems, where quinoa is a strategic crop for food security under variable climatic conditions [47]. Moderate deficit (Ks = 0.66) not only maintains but significantly improves quinoa productivity, challenging conventional irrigation paradigms that emphasize maximum water application [55]. In the central highlands, where rainfall is seasonal (concentrated January-March), and water availability is increasingly constrained, strategies optimizing water use efficiency while enhancing yield are critically needed to support sustainable agricultural intensification [54].

The rainfed treatment (365.4 mm effective rainfall vs. 520.6 mm ETo, generating 155.2 mm cumulative deficit) demonstrates that quinoa can thrive under seasonal limitations typical of highland environments [22]. This suggests cultivation in marginal areas with 350-400 mm seasonal rainfall may achieve superior productivity compared to over-irrigated systems, provided rainfall distribution allows adequate establishment before reproductive stages, consistent with observations that quinoa maintains or enhances performance under moderately restricted water availability in arid and semi-arid Andean environments [56, 57].

For irrigated systems, results support regulated deficit irrigation (RDI) strategies deliberately imposing moderate stress to improve water productivity [54]. Maintaining Ks around 0.65-0.70 could potentially double water productivity compared to full irrigation while enhancing protein content, offering substantial water savings without yield compromise. Spectral monitoring using NDVI, NDRE, and SRWI from UAV-mounted sensors offers practical tools for implementing precision deficit irrigation at field scale [18]. The clear differentiation among stress levels through these indices, detectable weeks before visible symptoms, enables timely irrigation adjustments to maintain crops within beneficial moderate stress zones. This multidimensional integration of spectral information can improve decision-making in high-Andean agricultural systems, where water variability and edaphoclimatic conditions make crop responses highly heterogeneous [51].

The patterns observed under moderate stress show that certain deficit levels can optimize water-use efficiency without compromising canopy optical integrity, consistent with recent reports demonstrating that crops can maintain spectral and physiological stability when stress does not exceed adaptive capacity [58]. This compensatory response opens opportunities to refine RDI strategies aimed at improving water productivity in resource-limited environments. The combination of morphological traits (compact architecture, well-developed panicles) with physiological traits (partial greenness maintenance, stable NDVI) observed at Ks = 0.66 may serve as useful selection criteria for breeding materials adapted to moderate water-stress scenarios typical of the central Andes [56, 59].

Quinoa in the central highlands is typically grown in rotation with tuber crops (potato, oca) or legumes (broad bean, tarwi) to reduce weed pressure and maintain soil fertility. The experimental site at Santa Ana Station followed this common rotation pattern, enhancing the practical applicability of results to smallholder farming systems. The substantial water productivity gains demonstrated under moderate deficit (Ks = 0.66), doubling grain production while saving 37% water, are therefore directly relevant to the rotational cropping systems predominant in the region, strengthening the feasibility of implementing deficit irrigation recommendations in farmer-managed landscapes.

4.5. Study Limitations and Future Research

Important considerations for interpreting and applying these results must be acknowledged. Constant water table lysimeters, while representing the most accurate method for quantifying crop water consumption and determining crop coefficients [30, 60], restrict lateral water movement and root exploration beyond the confined 1.2 m diameter soil volume. This differs from open-field conditions, where roots access broader soil profiles, and lateral water flow occurs. Extrapolating lysimeter-derived Kc values and water productivity relationships to heterogeneous field conditions requires consideration of spatial variability in soil properties, topography, and irrigation uniformity typical of commercial

Edelweiss Applied Science and Technology
ISSN: 2576-8484
Vol. 10, No. 3: 541-560, 2026
DOI: 10.55214/2576-8484.v10i3.12468

systems. Rain exclusion shelters, necessary for precise ETc measurement, may have introduced minor microclimate modifications despite transparent construction.

Single cultivar (INIA 433) evaluation during one growing season (January–June 2025) limits generalization across quinoa's substantial genetic diversity in stress response [48, 59]. The progressive deficit pattern observed (from April, affecting flowering/grain filling) represents one stress scenario; alternative timings may elicit different responses. Future research should address these limitations through: (1) multi-location field validation trials comparing deficit irrigation strategies across diverse Andean agroecological zones (2,500–4,000 m elevation); (2) multi-cultivar evaluations to identify genotypes consistently exhibiting beneficial responses to moderate deficit and elucidate underlying genetic mechanisms; (3) systematic manipulation of stress timing (vegetative, flowering, grain filling) and intensity (Ks = 0.5–0.8 range) to optimize deficit protocols for different phenological stages; (4) integration of spectral monitoring with direct physiological measurements (leaf water potential, stomatal conductance, photosynthetic rates) to mechanistically interpret remote sensing signals; (5) long-term studies evaluating deficit irrigation effects on soil health, residual fertility for subsequent rotation crops, and cumulative impacts over multiple seasons; and (6) participatory on-farm trials with smallholders to assess economic feasibility, labor requirements, and social acceptability of precision deficit irrigation technologies. Additionally, modeling approaches integrating climate projections with deficit irrigation strategies could inform adaptation planning for water-scarce Andean environments under future climate scenarios.

5. Conclusions

This study demonstrates that deficit irrigation substantially improves quinoa agronomic performance in the central highlands of Peru. Moderate water stress under rainfed conditions (Ks = 0.66) generated approximately 8,000 grains per plant, more than double that under optimal irrigation (Ks = 1.00, ~3,900 grains per plant), while increasing grain protein content from 4.8% to 6.0%. Moderate stress reduced evapotranspiration by 37% (374.5 to 234.4 mm) and doubled grain production, effectively quadrupling water use efficiency. In contrast, severe stress (Ks = 0.49) exceeded adaptive thresholds, reducing yield to 4,400 grains per plant and compromising quality. Multispectral indices (NDVI, NDRE, SRWI) effectively distinguished beneficial moderate stress from detrimental severe stress, offering practical tools for precision irrigation management. The water stress coefficient (Ks) proved an effective integrative metric linking soil water availability to crop performance. These findings have direct implications for water-scarce Andean systems, where seasonal rainfall (350-400 mm) can support superior productivity compared to over-irrigation. For irrigated systems, maintaining Ks around 0.65-0.70 offers potential to double water productivity while enhancing grain quality. Results demonstrate that quinoa cv. INIA 433 optimizes reproductive output under moderate water limitation, positioning deficit irrigation as a viable strategy for sustainable intensification in resource-limited Andean agroecosystems facing increasing water scarcity.

Funding:

This research was funded by the INIA project "Improving research and technology transfer services for the management and recovery of degraded agricultural soils and irrigation water in small and medium-sized farms in the departments of Lima, Áncash, San Martín, Cajamarca, Lambayeque, Junín, Ayacucho, Arequipa, Puno, and Ucayali" (CUI 2487112), of the Ministry of Agrarian Development and Irrigation (MIDAGRI) of the Peruvian Government. We would like to express our deepest gratitude to everyone who contributed to this research at the Santa Ana Experimental Station – Huancayo.

Transparency:

The authors confirm that the manuscript is an honest, accurate, and transparent account of the study; that no vital features of the study have been omitted; and that any discrepancies from the study as planned have been explained. This study followed all ethical practices during writing.

Copyright:

References

[1] G. Castorina *et al.*, "Maize landraces under water deficit favor diverse rhizosphere communities associated with improved stress response," *Rhizosphere*, vol. 36, p. 101200, 2025. https://doi.org/10.1016/j.rhisph.2025.101200

[2] M. Rahman *et al.*, "Integrating deep learning algorithms for forecasting evapotranspiration and assessing crop water stress in agricultural water management," *Journal of Environmental Management*, vol. 375, p. 124363, 2025. https://doi.org/10.1016/j.jenvman.2025.124363

[3] Q. Liu *et al.*, "Assimilating UAV observations and crop model simulations for dynamic estimation of crop water stress," *Agricultural Water Management*, vol. 318, p. 109688, 2025. https://doi.org/10.1016/j.agwat.2025.109688

[4] Y. Shi, X. Zhao, M. R. Tillotson, X. Zhang, R. Zhong, and H. Zhong, "Global water stress mitigation achieved through international crop trade," *Iscience*, vol. 28, no. 7, p. 112896, 2025. https://doi.org/10.1016/j.isci.2025.112896

[5] E. Zoratipour, S. Veysi, A. S. Mohammadi, S. B. Nasab, and A. A. Naseri, "Bias correction of satellite based crop water stress index using machine learning methods," *Agricultural Water Management*, vol. 320, p. 109862, 2025. https://doi.org/10.1016/j.agwat.2025.109862

[6] L. Albaladejo-Marico, M. Carvajal, and L. Yepes-Molina, "Priming with broccoli extract mitigates salinity stress in tomato through enhanced water and Na+/K+ homeostasis," *Journal of Plant Physiology*, vol. 314, p. 154612, 2025. https://doi.org/10.1016/j.jplph.2025.154612

[7] K. Buragohain, D. Tamuly, S. Sonowal, and R. Nath, "Impact of drought stress on plant growth and its management using plant growth promoting rhizobacteria," *Indian Journal of Microbiology*, vol. 64, no. 2, pp. 287-303, 2024. https://doi.org/10.1007/s12088-024-01201-0

[8] W. Luna-Flores, H. Estrada-Medina, E. Morales-Maldonado, and O. Á. Rivera, "Water deficit stress in plants: A review," *Chilean Journal of Agricultural & Animal Sciences*, vol. 31, no. 1, pp. 61-69, 2015.

[9] M. Peng, H. Yu, J. Huang, Y. Ren, and L. Fu, "Exacerbated global surface water stress under climate change," *Geography and Sustainability*, vol. 6, no. 6, p. 100361, 2025. https://doi.org/10.1016/j.geosus.2025.100361

[10] C. Corbari *et al.*, "High spatial resolution thermal infrared data from airborne acquisition reveal inconsistencies in evapotranspiration and crop water stress retrieval from different models," *Remote Sensing Applications: Society and Environment*, vol. 38, p. 101563, 2025. https://doi.org/10.1016/j.rsase.2025.101563

[11] J. Peng *et al.*, "Accurate estimates of land surface energy fluxes and irrigation requirements from UAV-based thermal and multispectral sensors," *ISPRS Journal of Photogrammetry and Remote Sensing*, vol. 198, pp. 238-254, 2023. https://doi.org/10.1016/j.isprsjprs.2023.03.009

[12] M. Ippolito, D. De Caro, G. Ciraolo, M. Minacapilli, and G. Provenzano, "Estimating crop coefficients and actual evapotranspiration in citrus orchards with sporadic cover weeds based on ground and remote sensing data," *Irrigation Science*, vol. 41, no. 1, pp. 5-22, 2023. https://doi.org/10.1007/s00271-022-00829-4

[13] B. Kamble, A. Kilic, and K. Hubbard, "Estimating crop coefficients using remote sensing-based vegetation index," *Remote Sensing*, vol. 5, no. 4, pp. 1588-1602, 2013. https://doi.org/10.3390/rs5041588

[14] H. Zhang *et al.*, "Crop coefficient determination and evapotranspiration estimation of watermelon under water deficit in a cold and arid environment," *Frontiers in Plant Science*, vol. 14, p. 1153835, 2023. https://doi.org/10.3389/fpls.2023.1153835

[15] S. Das *et al.*, "UAV-thermal imaging: A technological breakthrough for monitoring and quantifying crop abiotic stress to help sustain productivity on sodic soils–A case review on wheat," *Remote Sensing Applications: Society and Environment*, vol. 23, p. 100583, 2021. https://doi.org/10.1016/j.rsase.2021.100583

[16] J. W. Rouse, R. H. Haas, and J. A. Schell, "Monitoring vegetation systems in the Great Plains with ERTS," in *Proceedings of the Third Earth Resources Technology Satellite (ERTS) Symposium, Washington, D.C., USA*, 1973.

[17] A. A. Gitelson and M. N. Merzlyak, "Remote estimation of chlorophyll content in higher plant leaves," *International Journal of Remote Sensing*, vol. 18, no. 12, pp. 2691-2697, 1997. https://doi.org/10.1080/014311697217558

[18] P. J. Zarco-Tejada, C. Rueda, and S. Ustin, "Water content estimation in vegetation with MODIS reflectance data and model inversion methods," *Remote Sensing of Environment*, vol. 85, no. 1, pp. 109-124, 2003. https://doi.org/10.1016/S0034-4257(02)00197-9

Edelweiss Applied Science and Technology
ISSN: 2576-8484
Vol. 10, No. 3: 541-560, 2026
DOI: 10.55214/2576-8484.v10i3.12468

[19] M. Z. Akram, A. Libutti, and A. R. Rivelli, "Drought stress in quinoa: Effects, responsive mechanisms, and management through biochar amended soil: A review," *Agriculture*, vol. 14, no. 8, p. 1418, 2024. https://doi.org/10.3390/agriculture14081418
[20] D. Bazile, "Global trends in the worldwide expansion of quinoa cultivation," *Biology and Life Sciences Forum*, vol. 25, no. 1, p. 13, 2023. https://doi.org/10.3390/blsf2023025013
[21] M. Ghobadi and Z. Badehian, "Assessment of agricultural drought severity using multi-temporal remote sensing data in Lorestan region," *Scientific Reports*, vol. 15, no. 1, p. 18528, 2025. https://doi.org/10.1038/s41598-025-03087-4
[22] H. D. Bertero, A. De la Vega, G. Correa, S. Jacobsen, and A. Mujica, "Genotype and genotype-by-environment interaction effects for grain yield and grain size of quinoa (Chenopodium quinoa Willd.) as revealed by pattern analysis of international multi-environment trials," *Field Crops Research*, vol. 89, no. 2-3, pp. 299-318, 2004. https://doi.org/10.1016/j.fcr.2004.02.006
[23] S. M. Mirsafi, A. R. Sepaskhah, and S. H. Ahmadi, "Quinoa growth and yield, soil water dynamics, root growth, and water use indicators in response to deficit irrigation and planting methods," *Journal of Agriculture and Food Research*, vol. 15, p. 100970, 2024. https://doi.org/10.1016/j.jafr.2024.100970
[24] G. A.-. Nasser Salifu, "Synergies and trade-offs of sustainable agricultural practices for improved food security in a developing country: A systematic review," *Cogent Food & Agriculture*, vol. 11, no. 1, p. 2518218, 2025. https://doi.org/10.1080/23311932.2025.2518218
[25] A. N. Ralph, Q. Peter, T. E. Festus, A. N. Emmanuel, M. M. Butu, and H. N. Ellen, "Interlinkages between agri-food trade and the SDGs at the global, regional and local level," *Journal of International Development*, vol. 37, no. 4, pp. 951-977, 2025. https://doi.org/10.1002/jid.3994
[26] D. Ccopi *et al.*, "Using UAV images and phenotypic traits to predict potato morphology and yield in Peru," *Agriculture*, vol. 14, no. 11, p. 1876, 2024. https://doi.org/10.3390/agriculture14111876
[27] S. N. D. M. E. H. Senamhi, *Climate change scenario in the Mantaro River Basin by the year 2100*. Lima, Peru: Senamhi, 2010.
[28] Senamhi, "Report on dry and wet conditions in Peru during the hydrological year 2020-2021," 2021. https://scholar.googleusercontent.com/scholar?q=cache:_M5UVN90yYcJ:scholar.google.com/+condiciones+hidrológicas+del+Perú&hl=es&as_sdt=0,5
[29] FAO, "Quinoa growing guide," 2016. https://openknowledge.fao.org/server/api/core/bitstreams/76594aca-c6a8-45e0-97db-39905cd72575/content. [Accessed Dec. 18, 2025]
[30] R. G. Allen, "Crop evapotranspiration: Guidelines for computing crop water requirements," FAO Irrigation and Drainage Paper 56, Rome, Italy: Food and Agriculture Organization of the United Nations (FAO), 2000.
[31] R Core Team, "R: A language and environment for statistical computing, Version 4.x, Vienna, Austria: R Foundation for Statistical Computing," 2024. https://www.r-project.org/
[32] AOAC, *AOAC official method 2001.11: Protein (Crude) in animal feed, forage (Plant Tissue), grain, and oilseeds, in Official Methods of Analysis of AOAC International*. New York, USA: Oxford University Press, 2023.
[33] R. J. Hijmans, "Terra: Spatial data analysis, R package version 1.6-21," 2020. https://doi.org/10.32614/CRAN.package.terra
[34] QGIS Development Team, "QGIS geographic information system (Version 3.36) [Software]. Open Source Geospatial Foundation (OSGeo)," 2024. https://qgis.org
[35] R. G. Allen and L. S. Pereira, "Estimating crop coefficients from fraction of ground cover and height," *Irrigation Science*, vol. 28, no. 1, pp. 17-34, 2009. https://doi.org/10.1007/s00271-009-0182-z
[36] R. G. Allen, L. S. Pereira, D. Raes, and M. Smith, "Crop evapotranspiration: Guidelines for determining crop water requirements," FAO Riego y Drenaje Paper No. 56. Rome, Italy: Food and Agriculture Organization (FAO), 2006.
[37] F. Razzaghi, F. Plauborg, S.-E. Jacobsen, C. R. Jensen, and M. N. Andersen, "Effect of nitrogen and water availability of three soil types on yield, radiation use efficiency and evapotranspiration in field-grown quinoa," *Agricultural Water Management*, vol. 109, pp. 20-29, 2012. https://doi.org/10.1016/j.agwat.2012.02.002
[38] D. Raes, P. Steduto, T. C. Hsiao, and E. Fereres, "AquaCrop—the FAO crop model to simulate yield response to water: II. Main algorithms and software description," *Agronomy Journal*, vol. 101, no. 3, pp. 438-447, 2009. https://doi.org/10.2134/agronj2008.0140sDigital
[39] G. Grolemund and H. Wickham, "Dates and times made easy with lubridate," *Journal of Statistical Software*, vol. 40, no. 3, pp. 1-25, 2011. https://doi.org/10.18637/jss.v040.i03
[40] R. V. Lenth, "Emmeans: Estimated marginal means, aka least-squares means (R package version 1.8.5). Comprehensive R Archive Network (CRAN)," 2023. https://doi.org/10.32614/CRAN.package.emmeans
[41] H. Wickham, *ggplot2*. Cham: Springer International Publishing, 2016.
[42] H. Wickham *et al.*, "Welcome to the Tidyverse," *Journal of Open Source software*, vol. 4, no. 43, p. 1686, 2019. https://doi.org/10.21105/joss.01686
[43] H. Wickham, R. François, L. Henry, K. Müller, and D. Vaughan, "dplyr: A grammar of data manipulation (R package). Comprehensive R archive network (CRAN)," 2014. https://doi.org/10.32614/CRAN.package.dplyr
[44] R. Stikic *et al.*, "Agronomical and nutritional evaluation of quinoa seeds (Chenopodium quinoa Willd.) as an ingredient in bread formulations," *Journal of Cereal Science*, vol. 55, no. 2, pp. 132-138, 2012. https://doi.org/10.1016/j.jcs.2011.10.010

Edelweiss Applied Science and Technology
ISSN: 2576-8484
Vol. 10, No. 3: 541-560, 2026
DOI: 10.55214/2576-8484.v10i3.12468

[45] A. Yang, S. Akhtar, M. Amjad, S. Iqbal, and S. E. Jacobsen, "Growth and physiological responses of quinoa to drought and temperature stress," *Journal of Agronomy and Crop Science*, vol. 202, no. 6, pp. 445-453, 2016. https://doi.org/10.1111/jac.12167

[46] F. Tardieu, T. Simonneau, and B. Muller, "The physiological basis of drought tolerance in crop plants: A scenario-dependent probabilistic approach," *Annual Review of Plant Biology*, vol. 69, pp. 733-759, 2018.

[47] S.-E. Jacobsen, A. Mujica, and C. Jensen, "The resistance of quinoa (Chenopodium quinoa Willd.) to adverse abiotic factors," *Food Reviews International*, vol. 19, no. 1-2, pp. 99-109, 2003. https://doi.org/10.1081/FRI-120018872

[48] I. Maestro-Gaitán *et al.*, "Genotype-dependent responses to long-term water stress reveal different water-saving strategies in Chenopodium quinoa Willd," *Environmental and Experimental Botany*, vol. 201, p. 104976, 2022. https://doi.org/10.1016/j.envexpbot.2022.104976

[49] A. L. Gámez, D. Soba, Á. M. Zamarreño, J. M. García-Mina, I. Aranjuelo, and F. Morales, "Effect of water stress during grain filling on yield, quality and physiological traits of Illpa and Rainbow quinoa (Chenopodium quinoa Willd.) cultivars," *Plants*, vol. 8, no. 6, p. 173, 2019. https://doi.org/10.3390/plants8060173

[50] H. Dong *et al.*, "Crop water stress detection based on UAV remote sensing systems," *Agricultural Water Management*, vol. 303, p. 109059, 2024. https://doi.org/10.1016/j.agwat.2024.109059

[51] S. I. U. Haq *et al.*, "Multi-dimensional optical remote sensing in agriculture: Spectral, angular, and spatial scaling for crop stress monitoring," *Smart Agricultural Technology*, vol. 12, p. 101583, 2025. https://doi.org/10.1016/j.atech.2025.101583

[52] X. Zhang *et al.*, "Geospatial object detection on high resolution remote sensing imagery based on double multi-scale feature pyramid network," *Remote Sensing*, vol. 11, no. 7, p. 755, 2019. https://doi.org/10.3390/rs11070755

[53] M. González-Alcaraz, B. Aránega, H. Conesa, M. Delgado, and J. Álvarez-Rogel, "Contribution of soil properties to the assessment of a seawater irrigation programme as a management strategy for abandoned solar saltworks," *Catena*, vol. 126, pp. 189-200, 2015. https://doi.org/10.1016/j.catena.2014.11.012

[54] S. Geerts and D. Raes, "Deficit irrigation as an on-farm strategy to maximize crop water productivity in dry areas," *Agricultural Water Management*, vol. 96, no. 9, pp. 1275-1284, 2009. https://doi.org/10.1016/j.agwat.2009.04.009

[55] E. Fereres and M. A. Soriano, "Deficit irrigation for reducing agricultural water use," *Journal of experimental botany*, vol. 58, no. 2, pp. 147-159, 2007.

[56] L. Hinojosa, J. A. González, F. H. Barrios-Masias, F. Fuentes, and K. M. Murphy, "Quinoa abiotic stress responses: A review," *Plants*, vol. 7, no. 4, p. 106, 2018. https://doi.org/10.3390/plants7040106

[57] T.-H.-T. Nguyen *et al.*, "Tecomastane, a new megastigmane from the flowers of Tecoma stans," *Natural Product Research*, vol. 37, no. 21, pp. 3563-3571, 2023. https://doi.org/10.1080/14786419.2022.2092735

[58] Y. Zhang, T. Yu, W. Ma, C. Tian, Z. Sha, and J. Li, "Morphological and physiological response of Acer catalpifolium Rehd. Seedlings to water and light stresses," *Global Ecology and Conservation*, vol. 19, p. e00660, 2019. https://doi.org/10.3390/agronomy11051012

[59] W. Valdivia-Cea, L. Bustamante, J. Jara, S. Fischer, E. Holzapfel, and R. Wilckens, "Effect of soil water availability on physiological parameters, yield, and seed quality in four quinoa genotypes (Chenopodium quinoa Willd.)," *Agronomy*, vol. 11, no. 5, p. 1012, 2021. https://doi.org/10.3390/agronomy11051012

[60] H. Jung and M. Allen, "Characteristics of plant cell walls affecting intake and digestibility of forages by ruminants," *Journal of Animal Science*, vol. 73, no. 9, pp. 2774-2790, 1995.